JAAS

PAPER

View Article Online
View Journal | View Issue

Cite this: J. Anal. At. Spectrom., 2014, 29, 2078

Excitation and transition rate diagrams of singly ionized iron in analytical glow discharges in argon, neon and an argon–hydrogen mixture

Zdeněk Weiss,*[a] Edward B. M. Steers,[b] Juliet C. Pickering[c] and Sohail Mushtaq[b]

Received 28th June 2014
Accepted 19th August 2014

DOI: 10.1039/c4ja00214h

www.rsc.org/jaas

The emission spectra of iron observed using a Grimm-type glow discharge in argon, argon with 0.3% v/v hydrogen and neon were studied to identify major excitation and ionization processes of iron ions in the plasma. Transition rate diagrams are given for iron ions in those discharges. These are particularly useful for describing situations in which the rate of radiative decay of excited states is comparable to or exceeds the rate of their collisional de-excitation. Relationships between transition rate diagrams and Boltzmann plots are discussed. The following processes were identified to be responsible for excitation of Fe II glow discharge spectra: charge transfer from argon/neon ions to ground state- and metastable iron atoms, Penning excitation of ground state- and metastable iron ions by argon metastables and collisional excitation by electrons of metastable iron ions. No evidence was found that local thermodynamic equilibrium exists for iron ions in a glow discharge plasma in any interval of excitation energies. Open questions remain concerning charge transfer excitation of iron, in particular about the range of energies in which the Fe II levels can be directly populated by charge transfer and about the conservation of spin in such reactions.

1. Introduction

Emission spectra produced by analytical glow discharges[1,2] differ significantly from spectra generated by other common sources, such as ICP, spark, arc and laser-induced plasmas, reflecting different mechanisms that dominate the excitation and ionization of the analyzed elements.[3–5] The demand for a better understanding of excitation processes in analytical glow discharges has increased over the past decade after the introduction of CCD spectrometers that can measure emission spectra over wide continuous wavelength ranges, giving a large number of observed lines for most elements. To decide which lines are suitable for analysis of a given element in a given analytical application and to treat properly various excitation-related matrix effects[6] are other reasons for continuing work in this area.

There are two common methods that have been used in those studies so far: the first method is based on ratios of intensities of observed lines in a certain experiment and in another experiment with changed discharge conditions. The plot of these ratios as a function of excitation energy then reflects populations of different excited levels under the changed conditions relative to the populations under the 'reference' conditions, and is suitable to identify prospective selective excitation processes. This approach has been successfully used in glow discharge optical emission spectrometry (GD-OES) over the past *ca.* 30 years and led to great progress in understanding the role of selective excitation processes in analytical glow discharges[7–9] and also *e.g.* in ICP.[10] An advantage of using intensity ratios is that they are independent of the sensitivity function of the instrument used. However this approach has some serious drawbacks, *e.g.* that intensity ratios cannot be established for lines that do not exist (are not observed) in one of the two experiments, comparison of which is under study. The second most common approach assumes that the populations of various excited levels of an atom or ion under study reflects some kind of equilibrium maintained by collisions between those atoms and ions and other species in the plasma and investigates whether or to which extent the observed intensities reflect the Boltzmann distribution of those populations (the Boltzmann plot).[11–13]

Recently, a new formalism was proposed by Weiss *et al.*[14] to describe systematically radiative transitions occurring in emission spectra of an element and draw conclusions about the excitation processes involved. In this formalism, the rates of observed radiative transitions are evaluated and then plotted as functions of energy levels involved. Such plots are called transition rate diagrams (TR diagrams). These diagrams can yield more complete information about the observed spectra than either of the two methods mentioned above and do not depend

[a]LECO Instrumente Plzeň, spol. s r.o., Plaská 66, 323 25 Plzeň, Czech Republic. E-mail: weissz@leco.cz

[b]London Metropolitan University, 166-220 Holloway Road, London, N7 8DB, UK

[c]Blackett Laboratory, Imperial College London, Prince Consort Road, London, SW7 2AZ, UK

on any assumptions about the actual population distributions, such as assumptions utilizing the concept of the local thermodynamic equilibrium (LTE). This was demonstrated on the spectra of neutral and singly ionized manganese emitted by a Grimm-type glow discharge in argon, neon and an argon–hydrogen mixture.[14] To determine a TR diagram, the sensitivity function of the instrument used must be known and it is necessary to consider all observable lines, not only a narrow wavelength region. These conditions apply to the Boltzmann plots as well. The successful application of TR diagrams for manganese suggests the use of this approach also for other elements and this study is an attempt to do so for the glow discharge spectra of singly ionized iron. Besides its importance in analytical applications, iron was selected also because its electron structure is well known and a reliable classification of Fe II emission lines can be found in the literature.

The excitation of iron in glow discharges has been studied extensively in various experimental setups and under differing conditions.[8,9,11–13,15–22] This paper is an attempt to describe major excitation processes of ionized iron in analytical glow discharges as completely as possible, based on the formalism of TR diagrams. Besides argon, which is the most common

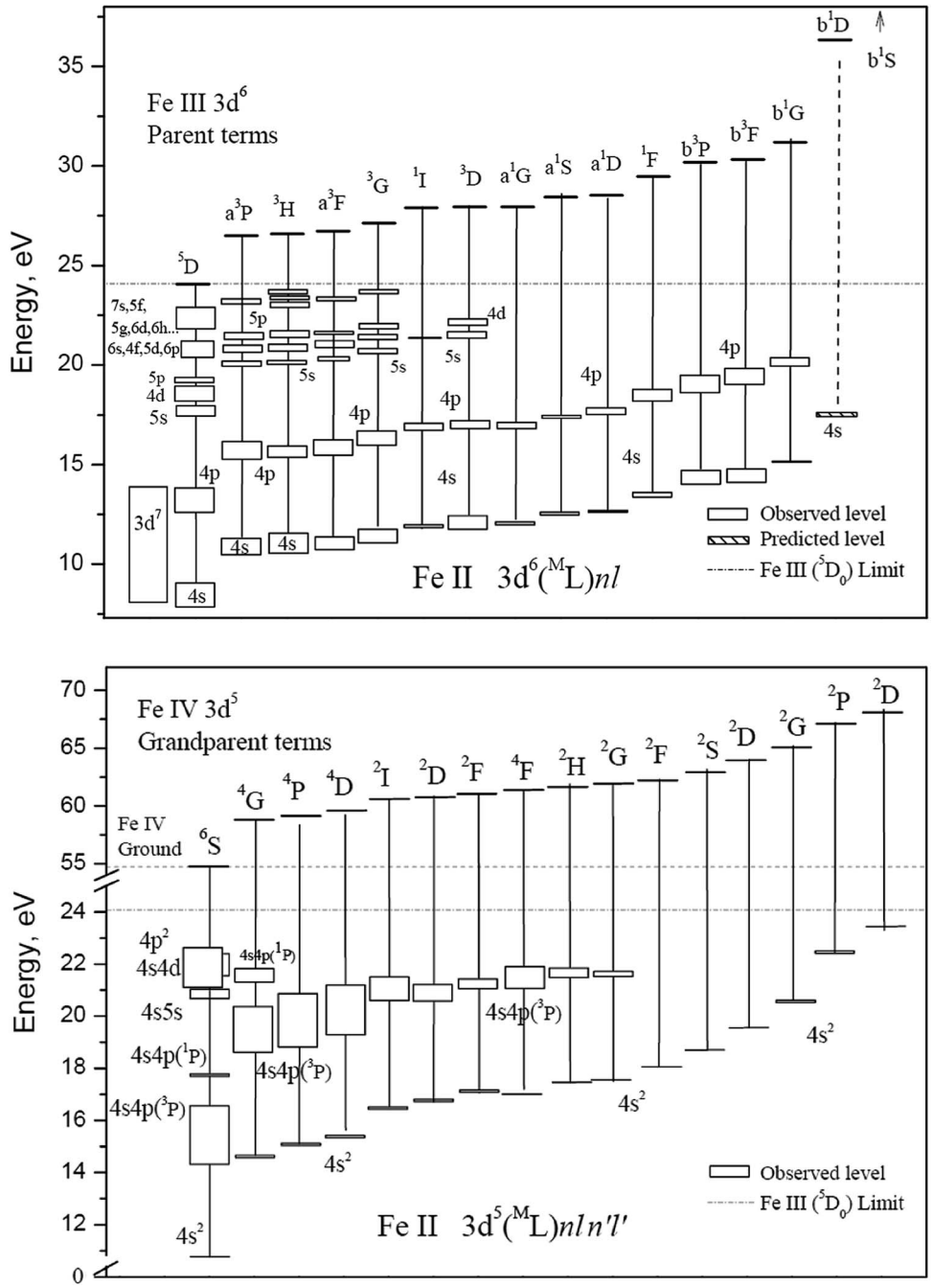

Fig. 1 Energy level structure of singly ionized iron. Top: the 'normal' system (singly excited) and bottom: the doubly excited system.

discharge gas in analytical applications, results for a discharge in neon are also included, to compare with an argon discharge and because discharges in neon may be useful in some situations. For a proper selection of analytical lines and interpretation of analytical data, it is often important to consider effects on emission spectra of hydrogen and other reactive gases, which may be present as impurities in the discharge gas or may come from the sample.[18,19] Therefore, results for a glow discharge in argon with a small addition of hydrogen are also described.

Iron is a transition element with a complex atomic structure that results from the partly filled 3d subshell. Fig. 1 shows schematic diagrams of the term structure of Fe II. The ground state term of the Fe ion is a sextet, $3d^6(^5D)4s\ a^6D$. The term structure of Fe II is formed by $3d^5\ nln'l'$, $3d^6\ nl$ and $3d^7$ systems. The singly excited ('normal') system is built on the $3d^6\ (^ML)\ nl$ set of configurations, where (^ML) is the associated parent term in Fe III, and nl is the valence electron that defines the orbital. In the term diagram the configurations are arranged according to their parent terms. Only the orbital configurations are labelled. The boxes represent the energy range of all the known levels in a given subconfiguration. The doubly excited system, $3d^5\ (^ML)\ nln'l'$, is built upon the grandparent terms $3d^5\ (^ML)$ in Fe IV. Many intermediate and high-lying levels in both the normal and doubly excited systems are affected by configuration mixing, giving more observed transitions than would be expected if LS selection rules were fully obeyed. A detailed description of the state of knowledge of the Fe II energy level system and spectrum can be found in Johansson[20] and Nave & Johansson,[21] where many newly identified lines and energy levels are reported.

2. Transition rate diagrams

The energy of a photon emitted in transition from level i to level j is $E_{ij} = E_i - E_j = hc/\lambda_{ij}$. The intensity of the spectral line is that energy multiplied by the number of transitions per second, n_{ij}, namely $I_{ij} = n_{ij}hc/\lambda_{ij}$. Hence the transition rate $n_{ij} = I_{ij}\lambda_{ij}/hc$ is proportional to the product $I_{ij}\lambda_{ij}$ of the intensity I_{ij} of the emission line associated with the transition $i \rightarrow j$ and its wavelength λ_{ij}. Transition rates associated with different emission lines can then be evaluated from the observed spectrum, except for a common multiplicative constant. In this sense, the quantities referred to as transition rates are transition rates expressed in some arbitrary units that are the same throughout the whole paper. In these considerations, it is supposed that the variations of instrument sensitivity with wavelength are known and corrected for, so that the "intensities" are on a uniform scale throughout. Every emission line in the spectrum starts at a certain excited level i and ends at a level j. Hence, level i is radiatively depopulated by the transition associated with this line and the level j is radiatively populated by that transition. Thus each level i is radiatively depopulated at a rate equal to the sum of the rates of all transitions associated with the lines of which i is the upper level. Similarly, a level is radiatively populated at a rate equal to the sum of the rates of the radiative transitions populating this level, *i.e.*, those transitions for which it is the lower level. As an example, this calculation is shown in Table 1 for the level $3d^6(^5D)4p\ z^6P_{3/2}^\circ$ of Fe II in a glow discharge in neon. In the upper part of the table, 10 transitions are listed, which populate this level by decay of higher excited states (cascade excitation), and in the lower part of the table 4 transitions which depopulate this level are listed. The rate of each transition (column 7) was calculated as the product $I_{ij}\lambda_{ij}$ of the intensity I_{ij} of the corresponding line and its wavelength λ_{ij}. Total excitation/de-excitation rates of this level are given in the final column. Because the de-excitation rate of this level is *ca.* 1.8 times higher than the rate of its cascade excitation, an additional excitation of this level by collisional processes must occur, because, under steady conditions of the discharge, excitation and de-excitation rates of each level must be equal. Total radiative excitation/de-excitation rates of different levels are then plotted as a function of their energy, where the de-excitation rates are represented by blue points as positive values, and the rates of radiative excitation by transitions from higher levels are represented by red points with values increasing downward, see Fig. 2. The resulting plot is called the TR diagram.[14] TR diagrams are particularly useful for studying excitation processes in low pressure plasmas such as glow discharges, in which lifetimes of most excited states are largely limited by radiative decay. In such situations, the rate of collisional excitation of a given state is equal to the difference between the rate of its radiative de-excitation and the rate of its radiative excitation, which can both be calculated from the emission spectrum. It should be noted that the formalism of TR diagrams, as presented above, gives an accurate picture only if the self-absorption of radiation can be neglected. Otherwise the true rates of radiative de-excitation would be higher than their estimates based on the measured line intensities.

Table 1 Calculation of radiative excitation/de-excitation rates of the Fe II level $3d^6(^5D)4p\ z^6P_{3/2}^\circ$ in a glow discharge in neon

		The level from/into[a]				Transition rate/arb. units	
λ_{ij}/nm	I_{ij}/arb. units	E^a/eV	Config.	Term	J	The line	Total
Transitions populating the $3d^6(^5D)4p\ z^6P_{3/2}^\circ$ level at 13.3108 eV							
286.412	0.087	17.6384	$3d^6(^5D)5s$	e^6D	5/2	103	8101
284.778	0.68	17.6632	"	"	3/2	783	
283.822	0.46	17.6779	"	"	1/2	511	
247.640	0.44	18.3159	$3d^6(^5D)4d$	^6D	3/2	133	
246.774	1.77	18.3335	"	"	1/2	572	
245.590	6.5	18.3577	"	^6P	5/2	2239	
245.003	5.6	18.3698	"	"	3/2	1756	
238.737	7.7	18.5025	"	^6S	5/2	1947	
158.701	0.094	21.1232	$3d^5 4s(^7S)4d$	^6D	3/2	25	
158.645	0.26	21.1260	"	"	5/2	68	
Transitions depopulating the $3d^6(^5D)4p\ z^6P_{3/2}^\circ$ level at 13.3108 eV							
232.740	13	7.9853	$3d^6(^5D)4s$	a^6D	5/2	3196	14 880
233.801	29	8.0094	"	"	3/2	7017	
234.429	19	8.0236	"	"	1/2	4521	
492.392	0.093	10.7935	$3d^5 4s^2$	a^6S	5/2	146	

[a] The upper level of transitions populating the level $3d^6(^5D)4p\ z^6P_{3/2}^\circ$ and the lower level of transitions depopulating the level $3d^6(^5D)4p\ z^6P_{3/2}^\circ$.

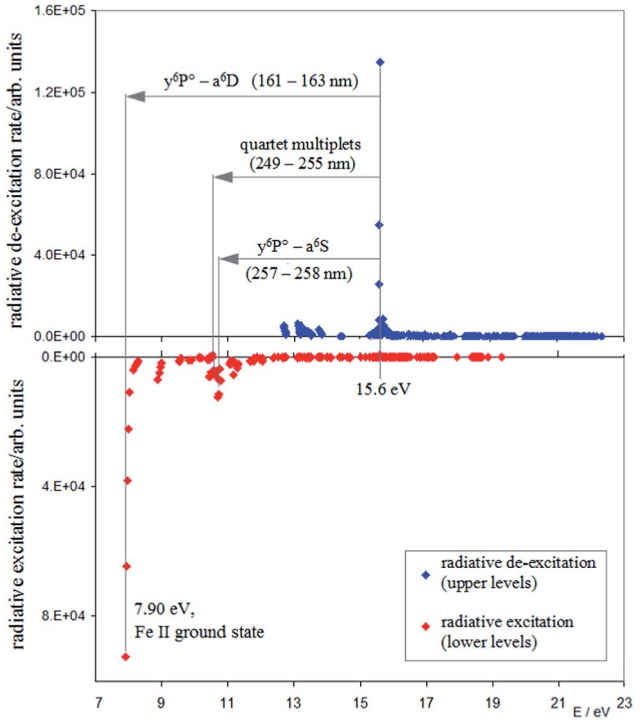

Fig. 2 TR diagram of Fe II in an argon discharge.

The ordinate scale in all TR diagrams in this paper is such that (relative) transition rates concern a certain amount of iron sputtered per second, *i.e.*, all transition rates throughout this paper are corrected for different sputtering rates in different discharge gases. Using the terminology common in analytical glow discharge spectroscopy, emission yields are used throughout this paper instead of raw intensities to calculate the rates of radiative transitions.[23] Therefore, the TR diagrams for argon-, argon–hydrogen and neon discharges in this paper can be compared on a quantitative basis.

3. Experimental details

The detailed analysis of the observed Fe spectra presented below is based on data from the vacuum-uv high resolution Fourier transform spectrometer (FTS)[24] at Imperial College London, used in conjunction with a free-standing Grimm-type source.[1] Three wavelength ranges were selected by choosing appropriate free spectral ranges and suitable photomultiplier tube detectors and, where needed, optical filters. The combined wavelength range of these FTS measurements was from 151 to 630 nm. The resolution used was: 0.035 cm^{-1} for the visible region (>365 nm); 0.05 cm^{-1} for the intermediate region (250–365 nm), and 0.07 cm^{-1} for the uv-vuv region (151–250 nm). This corresponds to a resolution of 0.14 pm at 200 nm. In another set of experiments, the wavelength range was extended up to 900 nm (not in a neon discharge). To obtain accurate relative line intensities, the areas under the line profiles were integrated. The calculation of transition rates mentioned above in Section 2 assumes that the intensities I_{ij} are 'true' intensities, corrected for sensitivity variations of the spectrometer used over the recorded spectral range. Hence, the radiometric calibration of the instrument, providing its sensitivity as a function of the wavelength, was necessary to obtain the corrected relative intensities. The radiometric calibration was performed using standard lamps, a tungsten–halogen lamp and a deuterium lamp, with known radiation characteristics,[25] and by the branching ratio method.[25] If a level has decay channels to more than one lower level, the decay is said to be 'branched'. The ratio $I_{ij}/I_{ij'}$ of intensities of radiation emitted in transitions from the same upper level i to lower levels j and j' is called the branching ratio and is given by the ratio of the corresponding transition probabilities divided by the wavelengths of those lines, $\lambda_{ij'}A_{ij}/(\lambda_{ij}A_{ij'})$, see ref. 25. By comparison of accurately established branching ratios with the actually measured intensity ratios, it is possible to calculate the ratios of the instrument sensitivities at the corresponding wavelengths. In this work, branching ratios in the Fe I (ref. 26–28) and Fe II (ref. 28 and 29) spectra were used to verify and complement the calibration data obtained using the standard lamps. The procedure will be described in more detail in a forthcoming paper on a new catalogue of glow discharge spectra. Work on the catalogue started some time ago[30] in the framework of the Analytical Glow Discharge Network "GLADNET",[31] a Marie Curie Research Training Network (RTN) funded by the EC under its Sixth Framework Programme (FP6). The results presented here are based on the Fe glow discharge spectrum to be published in this catalogue. Also, some software tools developed for the catalogue data were successfully used in this work. 1654 Fe II lines were identified in the spectrum (638 in an argon discharge and 1501 in a neon discharge) and 519 levels were considered to construct the TR diagrams. The classification of the lines is based on the NIST database[28] and the work by Nave and Johansson.[21] Excitation energies in the Fe II spectrum are given relative to the ground state of the Fe atom throughout this paper. They differ from excitation energies relative to the ground state of the Fe^+ ion, more usually listed in the tables, by the ionization energy of iron, $E_i = 7.9024$ eV.

In addition to the FTS measurements, some complementary data were collected using the LECO GDS500A GD-OES spectrometer,[32] a grating instrument with CCD detection, with a resolution of 60–70 pm and a wavelength range of 165–465 nm, in the LECO European Technical Centre, Prague. These data were particularly useful in investigations of the effects of a small addition of hydrogen to the argon discharge gas on the Fe II spectra, described in Section 4.3 in this paper, in the vacuum ultraviolet wavelength region below 200 nm.

All the experiments were carried out under 'standard' operating conditions of the glow discharge, *i.e.* a dc discharge with a 4 mm internal diameter anode, with constant voltage–constant current stabilization at 700 V, 20 mA. The spectra of iron were collected using a 99.9% pure Fe sample. The discharge gas was argon, neon or argon with added hydrogen at the level of 0.3% v/v, below referred to as an Ar(H) mixture. The pressure of the working gas under the discharge conditions mentioned above was 5.6 Torr for a discharge in argon and 12.7 Torr for a discharge in neon.

4. Results and discussion

4.1. Fe II spectrum in an argon discharge

The TR diagram of Fe II in an argon discharge is shown in Fig. 2. The most prominent peak in the upper side of the diagram at ≈15.6 eV corresponds to de-excitation of the Fe II levels populated by asymmetric charge transfer (ACT) reaction between neutral iron atoms and argon ions, see *e.g.* ref. 8 by Steers *et al.*:

$$Fe^0 + Ar^+ \rightarrow Fe^{+}{}^{*} + Ar^0 + \Delta E \quad (1)$$

ACT is a resonant process, selectively populating Fe II levels that are close to the energy of Ar ions (15.76 eV and 15.94 eV for the metastable $Ar^{+}{}^{*}$ $^2P_{1/2}$ ion), so that ΔE is a small positive or negative value. Also, the preservation of the total spin of the reacting species is assumed for an ACT reaction.[8] This leads to excitation of Fe II quartets and sextets because the ground state term of the Fe atom is a quintet. The most strongly excited Fe II levels by Ar^+-ACT are those belonging to a sextet term, $3d^5(^6S)4s4p(^3P)\,y^6P^\circ$, (15.59–15.61 eV). Their radiative decay dominates the TR diagram in Fig. 2, populating levels belonging to the Fe II ground term (the y^6P°–a^6D multiplet, λ = 161–163 nm, marked in the TR diagram in Fig. 2) and also levels of the $3d^54s^2\ a^6S$ term at ≈10.79 eV (y^6P°–a^6S, λ = 257–258 nm). Close to the sextet term are quartet terms with strong transitions between the levels at 15.50–15.55 eV and 10.53–10.75 eV, λ = 249–255 nm. However, the TR diagram in Fig. 2 shows only a very rough outline of the situation and a more detailed view can be obtained by plotting the transition rates on a logarithmic scale and by distinguishing the multiplicities of the levels by different colours of the corresponding points. Such a modified TR diagram is shown in Fig. 3.

In the Fe II spectrum in an argon discharge, not many levels are subjected to cascade processes (excitation by decay of higher excited levels followed by radiative de-excitation) and for those that are subjected to cascade processes, the observed rates of

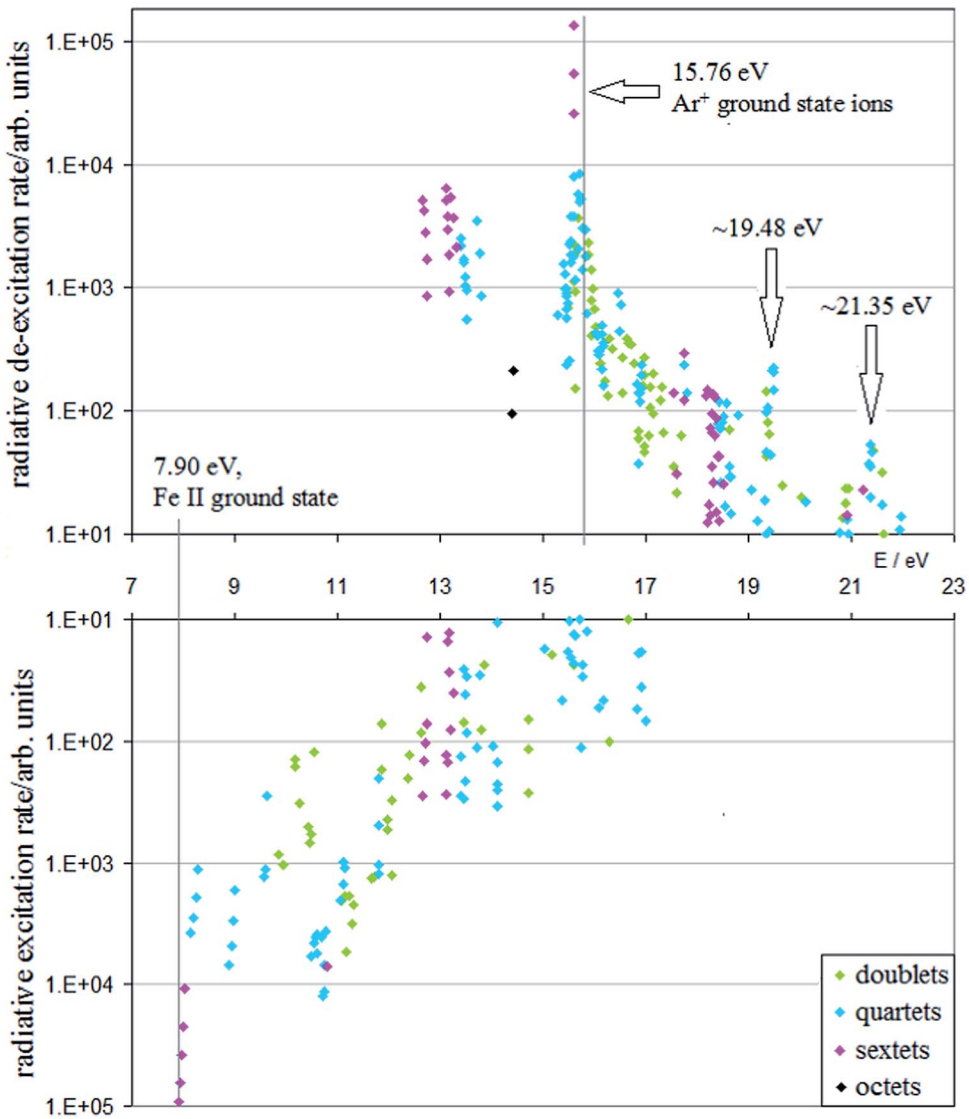

Fig. 3 TR diagram of Fe II in an argon discharge, logarithmic ordinate scale.

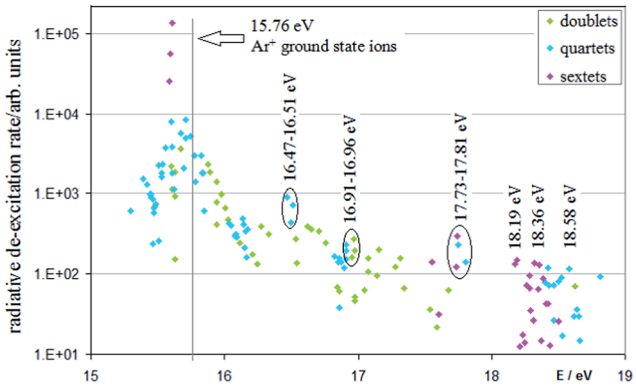

Fig. 4 Radiative de-excitation rates in an argon discharge of Fe II levels with energies between 15 eV and 19 eV (note a logarithmic ordinate scale).

cascade excitation are small compared to their de-excitation rates. Hence, it is very likely that, for most levels, the de-excitation rates in the upper part of the TR diagram in Fig. 3 reflect well their collisional excitation. Concerning the charge transfer reaction mentioned above, levels of the sextet term $3d^5(^6S)$ $4s4p(^3P)$ y^6P° are more strongly excited than the nearby quartet Fe II levels with a similar energy: their de-excitation rates are higher by an order of magnitude. A stronger excitation of the sextet levels mentioned above than the nearby quartet levels was observed also by Zhang *et al.*[13] If this behaviour is related to the term multiplicity (there are no other Fe II sextet terms with energy suitable for Ar^+-ACT), it means that the parallel orientation of the spins of the reacting particles is preferred over the anti-parallel. Some quartet levels just above the argon ionization energy are also excited, with the excitation rates falling off as the energy difference increases. An expanded portion of the TR diagram between 15 eV and 19 eV is shown in Fig. 4. It shows that also some doublet Fe II levels with energies close to the argon ionization energy are excited. It is unclear how these are excited, as the total spin would not be preserved if they were excited by Ar^+-ACT. Further discussion of Fe II levels excited by Ar^+-ACT is in Section 4.4 below, in comparison with a neon discharge.

The two octet levels at ≈14.4 eV in Fig. 3 with low de-excitation rates belong to the term $3d^5(^6S)4s4p(^3P^\circ)$ z^8P°, are partly metastable and decay by inter-combination transitions to the levels of the ground state Fe II term, $3d^6(^5D)4s$ a^6D (a sextet). Therefore, the corresponding transition probabilities are probably low and the populations of these levels are most likely controlled by collisional processes (the positions of the corresponding points in the TR diagram in Fig. 3 do not reflect the rate of their collisional excitation).

From the diagram in Fig. 3, it is apparent that there are also excited levels with relatively high energies, although these are much less excited than levels with energies close to 15.6 eV and lower, and there is a clear trend showing a decrease of (collisional) excitation rates with increasing energy. Exceptions to this rule are two well pronounced peaks at ≈19.48 eV and ≈21.35 eV. The first of these consists of transitions involving two quartet terms, $3d^6(^3F1)4p$ u^4F° and $3d^6(^3F1)4p$ $^4D^\circ$, at 19.47–19.49 eV, and most likely reflects the Penning excitation of Fe^+ ground state ions by Ar metastables ($E \approx 11.55$ eV):

$$Fe^+[3d^6(^5D)4s\ a^6D] + Ar^*[3s^23p^5(^2P_{3/2}^\circ)4s\ ^3P_2] \rightarrow Fe^{+*}[3d^6(^3F1)4p\ u^4F^\circ] + Ar\ [3s^23p^6\ ^1S_0] + \Delta E \quad (2)$$

$$Fe^+[3d^6(^5D)4s\ a^6D] + Ar^*[3s^23p^5(^2P_{3/2}^\circ)4s\ ^3P_2] \rightarrow Fe^{+*}[3d^6(^3F1)4p\ ^4D^\circ] + Ar\ [3s^2\ 3p^6\ ^1S_0] + \Delta E \quad (3)$$

These reactions have a resonant character and exhibit a perfect energy match, with $\Delta E = 0.02$–0.03 eV. Also spin is conserved.

The peak at ≈21.35 eV in the TR diagram shown in Fig. 3 consists of transitions involving the ^4D, ^4G, ^4H, ^4I terms, all with the same subconfiguration, $3d^6(^3G)4d$. In a search for possible energy resonances, it was found that these levels can be excited by Penning excitation of Fe^+ metastables with energies of 9.57–9.63 eV ($3d^7\ a^4P$) in collisions with argon metastables with an energy of 11.72 eV, $3s^23p^5(^2P_{1/2}^\circ)4s\ ^3P_0$:

$$Fe^+[3d^7\ a^4P] + Ar^*[3s^23p^5(^2P_{1/2}^\circ)4s\ ^3P_0] \rightarrow Fe^{+*}[3d^6(^3G)4d\ ^4X] + Ar\ [3s^23p^6\ ^1S_0] + \Delta E \quad (4)$$

where ^4X means one of the ^4D, ^4G, ^4H, ^4I terms. The $3d^7\ a^4P$ metastable levels of Fe^+ are (weakly) populated by radiative de-excitation of several higher Fe^+ levels, with the total cascade excitation rate of the $3d^7\ a^4P$ term of $\approx 2.7 \times 10^3$ units (see the three quartet levels at *ca.* 9.6 eV in the bottom part of the TR diagram in Fig. 3). This would be sufficient to balance the loss of these metastables by the Penning reaction (eqn (4)) mentioned above, as the combined de-excitation rate of the Fe^+ levels at ≈21.35 eV is only 2.4×10^2. Moreover, the $3d^7\ a^4P$ term is only ≈1.7 eV above the ground state of the Fe^+ ion and collisions of ground state Fe^+ ions with electrons are likely to contribute significantly to the creation of these metastables.

In the energy range between the levels excited presumably by Ar^+-ACT with ground state Fe atoms, reaction (1), and the peak corresponding to the Penning excitation of Fe^+ ions by reactions (2) and (3), there are a number of levels with radiative de-excitation rates between 10^2 and 10^3 (see the TR diagram in Fig. 3 and 4). Excitation of these levels can occur by charge transfer between Ar^+ ions and metastable (excited) iron atoms, *i.e.*, by the reactions (5) and (6) below:

$$Fe^*(m) + Ar^+[3p^5\ ^2P_{3/2}^\circ] \rightarrow Fe^{+*} + Ar^0 + \Delta E \quad (5)$$

$$Fe^*(m) + Ar^{*+}[3p^5\ ^2P_{1/2}^\circ] \rightarrow Fe^{+*} + Ar^0 + \Delta E \quad (6)$$

while the reaction (5) involves ground state argon ions ($3p^5\ ^2P_{3/2}^\circ$, $E = 15.76$ eV) and reaction (6) involves the $3p^5\ ^2P_{1/2}^\circ$ metastable argon ions ($E = 15.94$ eV). The iron atom has a number of metastable states, the transitions of which to the Fe I ground state ($3d^64s^2\ a^5D_4$) are either parity-forbidden or spin-forbidden or both. In the plot shown in Fig. 4, several groups of states are marked, of which higher de-excitation rates were observed than in their vicinity. The sextet states at ≈15.6 eV are excited by Ar^+-ACT with ground state Fe atoms, reaction (1), as discussed

Table 2 Possible excitation of some Fe II states by ACT between Ar^+ ions and Fe metastable atoms (reactions (5), (6)): energy decrements ΔE in eV

		Excited Fe II levels observed in emission spectra						
		E/eV	16.47–16.51	16.91–16.96	17.73–17.81	18.19	18.36	18.58
		2S + 1	4	2, 4	4, 6	6	6	4
Fe I metastables								
		E/eV						
$3d^7(^4F)4s$	a^5F	0.85–1.00	0.12					
"	a^3F	1.49–1.61		(0.29)				
$3d^7(^4P)4s$	a^5P	2.17–2.22			0.16			
$3d^6(^5D)4s4p(^3P^\circ)$	z^7D°	2.40–2.48				−0.03, 0.15[a]		
$3d^7(^2G)4s$	a^3G	2.69–2.73						0.05[a]
$3d^6(^5D)4s4p(^3P^\circ)$	z^7F°	2.81–2.89					0.21	
$3d^7(^4P)4s$	b^3P	2.83–2.86						0.01, 0.19[a]

[a] This energy decrement corresponds to a reaction with argon metastable ions (15.94 eV).

above. The other groups of states marked in Fig. 4 are listed in Table 2, rows 2 and 3, together with their energies and spin multiplicities (2S + 1). For these groups of states, charge transfer reactions of the type (5) and (6) were found that are likely to be responsible for their excitation: the corresponding energy decrements ΔE are sufficiently small and multiplicities of those states are such that the total spin in these reactions is conserved. Such reactions are represented by the corresponding energy decrements and listed in Table 2. Reactions with argon metastable ions, eqn (6), are specified by the sign *, referring to a remark under the table, and all other suggested reactions are of the type (5), with argon ground state ions. Table 2 shows the terms of Fe I, not individual metastable levels. Each energy decrement ΔE in Table 2 corresponds to an ACT reaction with Fe atoms in the state with the lowest energy in the term, which has also the highest quantum number J and thus the highest statistical weight. One more remark to be made is that the combined de-excitation rate of all levels presumably excited by Ar^+-ACT (E = 15.4–18.6 eV) is ≈82% of the total de-excitation rate of all observed Fe II transitions and the combined de-excitation rate corresponding to Ar^+-ACT with the ground state Fe atoms only (15.4–15.9 eV) is ≈77%. This means that ≈4/5 of all photons in the Fe II spectrum in an argon discharge come from Fe ions created by the Ar^+-ACT reaction.

What remains to be discussed are the Fe II levels between 12.6 and 13.8 eV. Transitions involving these levels exhibit a very similar pattern in argon and neon discharges. The Fe II TR diagram for a glow discharge in neon is shown in Fig. 5: see the quartet and sextet levels around 13 eV in the upper part of the diagram and compare with those levels in the TR diagram for an argon discharge shown in Fig. 3. Therefore, in the following section, excitation of those levels in both discharge gases is discussed together.

4.2. Fe II levels between 12.6 and 13.8 eV in argon and neon discharges

Because excitation of those levels in both discharge gases is similar, the excitation mechanism will not be a selective one, tied to a certain characteristic energy of argon or neon. Zhang *et al.* reported[13] that populations of these levels in an argon discharge follow the Boltzmann distribution with a temperature of ≈6500 K. This would imply that conditions close to local thermodynamic equilibrium (LTE)[25] should exist for those levels. To confirm or dismiss this hypothesis, excitation functions in this energy region were determined also from our data, both for argon and neon discharges (see Fig. 6 and 7). The Boltzmann distribution[25] can be expressed as

$$\frac{n_2}{n_1} = \frac{g_2}{g_1} \mathrm{e}^{\frac{-\Delta E}{kT}} \quad (7)$$

where n_1 and n_2 are the populations of two atomic or ionic levels with excitation energies E_1 and E_2 and statistical weights g_1 and g_2, T is the excitation temperature, k is the Boltzmann constant and $\Delta E = E_2 - E_1$. The intensity I_{ik} of a line corresponding to a transition $i \rightarrow k$ is

$$I_{ik} = n_i A_{ik} \frac{hc}{\lambda_{ik}} \quad (8)$$

where A_{ik} is the transition probability, λ_{ik} is the wavelength of that line, h is the Planck constant, c is the speed of light and n_i is the population of the upper level i of that transition. In a Boltzmann plot, the quantity $hcn_i/g_i = \lambda_{ik}I_{ik}/g_iA_{ik}$ is plotted as a function of energy E_i, on a logarithmic scale. Such a plot may not be necessarily linked to a certain Boltzmann distribution and can be understood in a more general meaning simply as the excitation function plotted with a logarithmic ordinate scale. As such, it is a legitimate tool for studying general population distributions. It should be noted that only if the points in such a plot were to follow a straight line with a negative slope, can it be inferred that the plot reflects some kind of thermodynamic equilibrium, with temperature inversely proportional to the slope of that line. Excitation functions derived from our data are shown in Fig. 6 and 7 and do not exhibit such a feature. The dashed line shown in Fig. 6 is only to show what Zhang *et al.* reported to be a good linear fit to their data[13] and is not a linear fit to our data. Zhang *et al.* worked with different discharge parameters (a 8 mm diameter anode, 800 V, 30 mA) and used

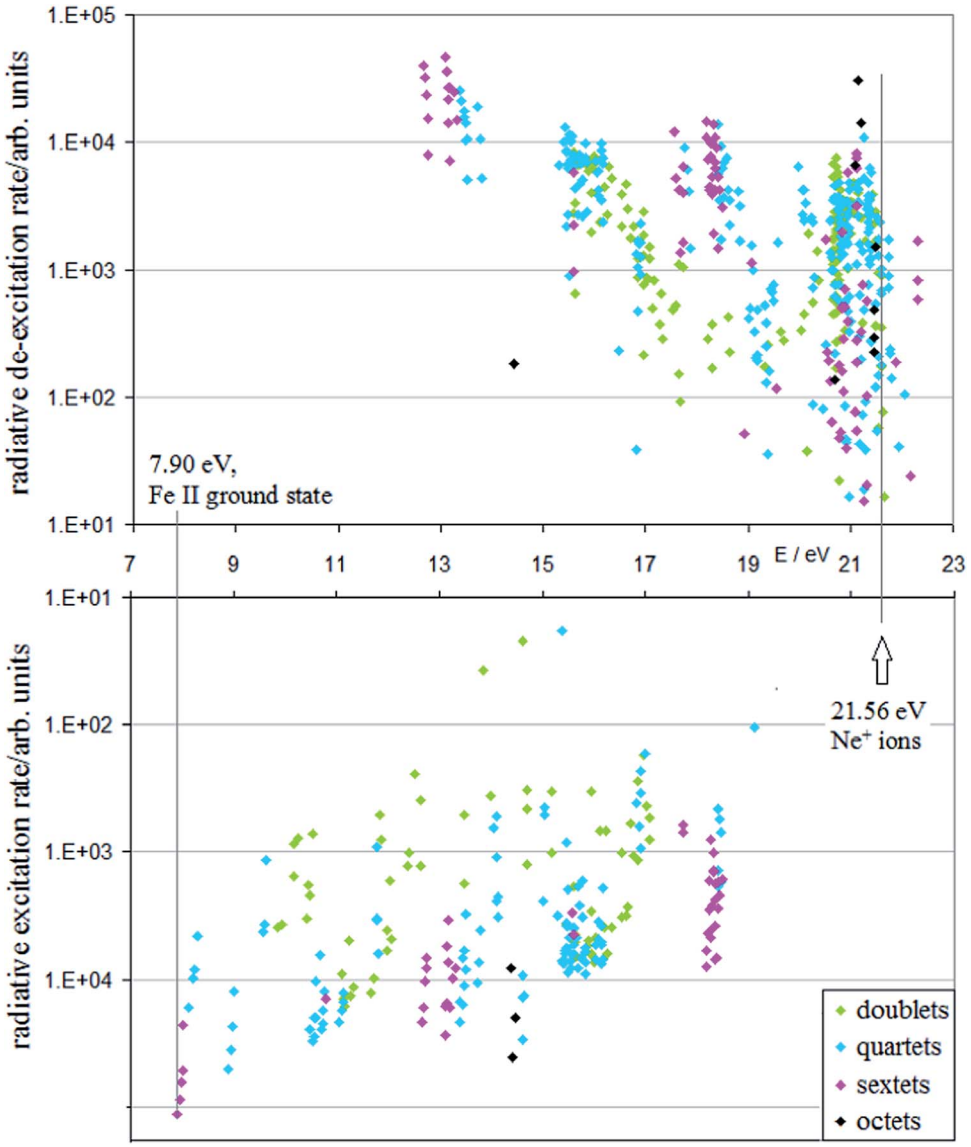

Fig. 5 TR diagram of Fe II in a neon discharge.

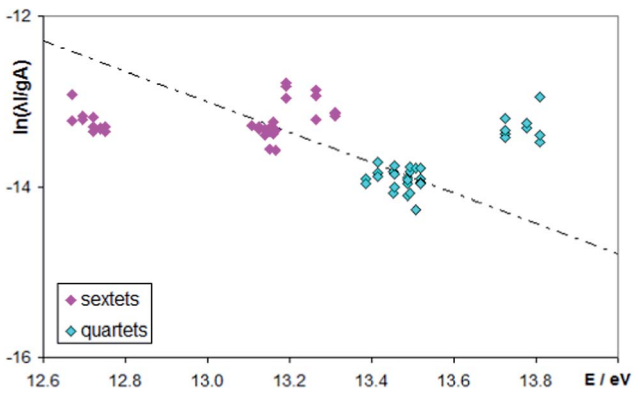

Fig. 6 Excitation function for Fe II lines with excitation energies of 12.6–13.8 eV in an argon discharge. The dashed line is not a linear fit to these data but its gradient corresponds to the "temperature" quoted in ref. 13.

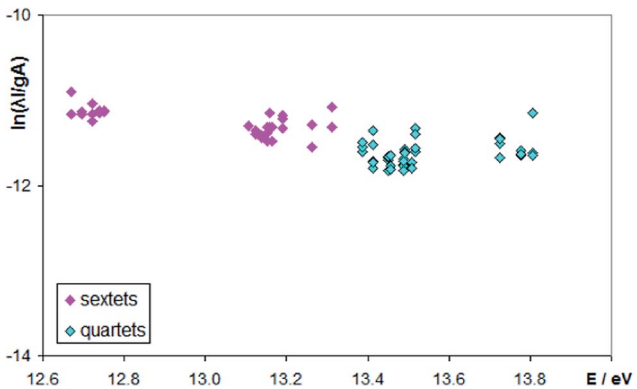

Fig. 7 Excitation function for Fe II lines with excitation energies of 12.6–13.8 eV in a neon discharge.

fewer lines, spanning over a narrower wavelength range to avoid the need for determining the change with the wavelength of the sensitivity of their instrument. Transition probabilities used to calculate the excitation functions in Fig. 6 and 7 were taken from the work by Fuhr and Wiese.[33] From the plots in Fig. 6 and 7 it is apparent that the level populations do not follow a clear trend as a function of energy and any 'temperature' based on a certain limited group of lines is meaningless. Probably the most appropriate statement about these excitation functions is that they do not depend much on energy in this region, certainly not in a way that would justify the introduction of a 'temperature' in the order of 10^3–10^4 K. The points shown in Fig. 7 are less scattered than those shown in Fig. 6. This is probably because the corresponding lines are much stronger in a neon discharge than in argon ($\approx$10 times) and the uncertainty associated with the measured intensities is thus smaller. It is difficult to estimate the uncertainties of individual points in both plots. Some considerations of this kind will be given in the forthcoming paper on a new catalogue of glow discharge spectra, mentioned above in Section 3.

The Fe^+ ion has a number of metastable states between $\approx$10.7 eV and 12.6 eV, the radiative decay of which is parity-forbidden and which belong *e.g.* to the following terms: a sextet, $3d^5 4s^2\ a^6S$ (10.79 eV), a number of quartets (up to 11.1 eV) and a number of doublets, up to 12.6 eV. These metastable levels are populated by radiative decay of higher excited states (see the lower part of the TR diagrams in Fig. 3 and 5) and presumably also by collisions of electrons with Fe^+ ions. A hypothesis may be suggested that collisions with electrons of these metastables contribute significantly to the excitation of the Fe II levels between 12.6 and 13.8 eV investigated here. For LTE to exist for these states, the electron density would have to be sufficiently high to prevent the would-be collisional equilibrium with electrons from being perturbed by radiative decay of these states.[25] That is apparently not the case here, as follows from the excitation functions in Fig. 6 and 7.

4.3. Fe II spectrum in an argon–hydrogen discharge

A TR diagram of Fe II in an Ar(H) discharge is shown in Fig. 8. Compared with the TR diagram for a discharge in pure argon (Fig. 3), the most apparent feature is that the peak at $\approx$15.6 eV and vicinity, corresponding to the Ar^+-ACT reaction, is greatly suppressed, whilst the other groups of states are either not suppressed or suppressed to a much lesser extent. Many weak lines from the discharge in argon were not observed in the Ar(H) discharge, which is the reason why many Fe II levels with low de-excitation rates, displayed in Fig. 3, are missing in Fig. 8. A clearer picture is shown in Fig. 9 in which ratios of de-excitation rates in Ar- and Ar(H) discharges are plotted with a linear ordinate scale as a function of energy of the Fe II levels. As mentioned above, transition rates are corrected for a different sputtering rate of iron in both discharges, by a factor $q_{Ar(H)}(Fe)/q_{Ar}(Fe) = 0.77$.[18,34] Hence, in an approximation of negligible collisional de-excitation, the plot in Fig. 9 can be interpreted as the relative probability of a level to be excited in an Ar(H) discharge, compared to an argon discharge. The plot shown in

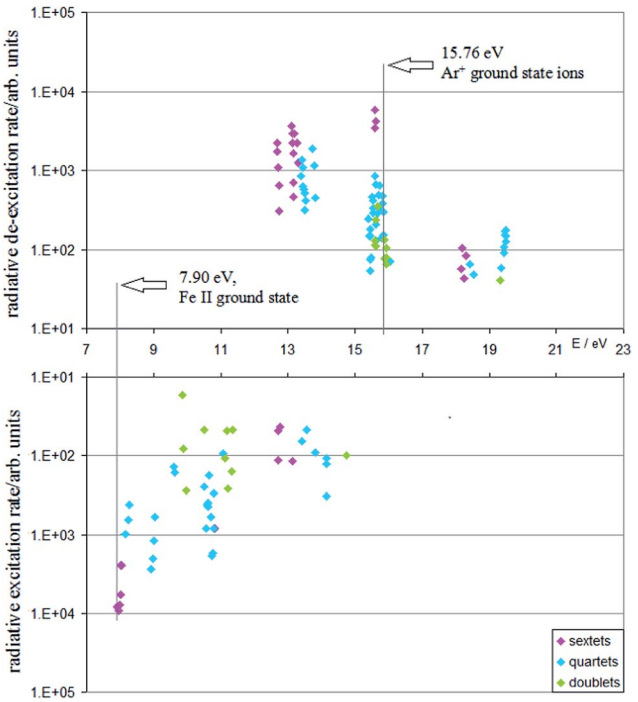

Fig. 8 TR diagram of Fe II in an argon–hydrogen discharge.

Fig. 9 is in good agreement with the results described by Steers *et al.*[18] and gives more information than ref. 18 for levels above 18 eV. The Ar(H)/Ar factors of $\approx$0.15–0.25 were observed for all levels that are close to 15.6–15.8 eV, including the doublet levels. Hydrogen greatly reduces the population of Ar^+ ions, creating ArH^+ ions instead[35] and reducing thereby the rate of the Ar^+-ACT reactions in the discharge.[36] This is the case here. It is remarkable that the Fe II *doublet* levels that are close to the resonance energy for Ar^+-ACT also behave in the same manner as the quartet and sextet levels for which the Ar^+-ACT reaction preserves the spin. The levels between 12.6 and 13.8 eV, described earlier under Section 4.2, split into two groups, of which the sextet levels, with lower energies, are suppressed and the quartet levels are not. They exhibit a peak in the vicinity of 13.6 eV, the ionization energy of hydrogen. This behaviour was

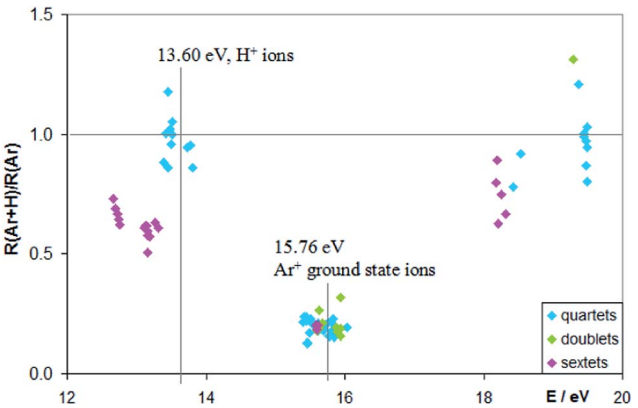

Fig. 9 TR(Ar + H)/TR(Ar) enhancement factors for Fe II levels.

also described by Steers *et al.*[18] and attributed to charge transfer reaction between iron atoms and H^+ ions.

The Fe II levels around 18 eV, excited presumably by Ar^+-ACT with iron metastables (Table 2) are also slightly suppressed in an Ar(H) discharge but less than those around 15.6–15.8 eV mentioned above. Finally, most of the levels around 19.5 eV excited by Penning excitation of Fe^+ ions by argon metastables, eqn (2) and (3), are virtually unaffected by the addition of hydrogen. Lines associated with transitions from those levels are weak (see Fig. 3), which causes increased uncertainties of the measured intensities and the scatter of the points around 19.5 eV in Fig. 9.

4.4. Fe II spectrum in a neon discharge

A TR diagram of Fe II in a neon discharge is shown in Fig. 5 and an initial discussion of its implications is given in this section. As in the case of the Ar(H) discharge, transition rates were corrected for a different sputtering rate of iron in argon and neon discharges, with a factor $q_{Ne}(Fe)/q_{Ar}(Fe) = 0.45$, and the TR diagrams for argon and neon discharges in this paper can thus be compared on a quantitative basis. One result that can be derived from such a comparison is *e.g.* that the combined de-excitation rate corresponding to all observed transitions in the spectrum (*i.e.* the number of emitted photons per certain number of sputtered iron atoms) is 3.9×10^5 units in an argon discharge and 1.8×10^6 in neon, *i.e.*, 4.6 times bigger.

The excitation of the low-energy Fe II states at ≈12.6–13.8 eV was discussed in Section 4.3. The ionization energy of neon is 21.56 eV and the difference between the TR diagrams in argon (Fig. 3) and neon (Fig. 5) suggests that the Ne^+-ACT reaction with iron plays a very significant role in populating Fe II levels above *ca.* 20.6 eV. A large number of levels with de-excitation rates $>10^3$ spans from ≈20.6 to 21.6 eV, which is a much wider interval than the width of the peak in the TR diagram in Fig. 3, corresponding to the Ar^+-ACT reaction. We observed a similar phenomenon for manganese.[14] An expanded section of the Fe II TR diagram in a neon discharge, spanning the energy range from 19 to 23 eV, is shown in Fig. 10, together with a diagram depicting energies of all existing Fe II levels in that interval, sorted by their spin multiplicity. It is remarkable that the strongly excited levels also include some octet states at 21.1–21.5 eV, close to the resonance energy for Ne^+-ACT, but not compatible with the requirement of spin conservation in the Ne^+-ACT reaction with ground state Fe atoms. This particularly concerns the $3d^5(^6S)4p^2\ ^8P$ term at 21.1–21.2 eV. A closer look shows that all existing Fe II octet states within a ≈1eV-wide energy interval below the ionization energy of neon are excited, whilst the levels that are closer to the neon ionization energy, belonging to the term $3d^54s(^7S)4d\ ^8D$ (21.47 eV), are much less excited than those at 21.1–21.2 eV ($3d^54p^2\ ^8P$). Also, there are a number of doublet levels, relatively strongly excited, in that energy range. They also do not comply with the Wigner spin rule for direct Ne^+-ACT reaction with ground state Fe atoms. Many of them decay by inter-combination transitions to sextet levels at 18.2–18.4 eV, with the wavelengths of the corresponding lines around 500 nm. A notable feature in the plot shown in Fig. 10 is

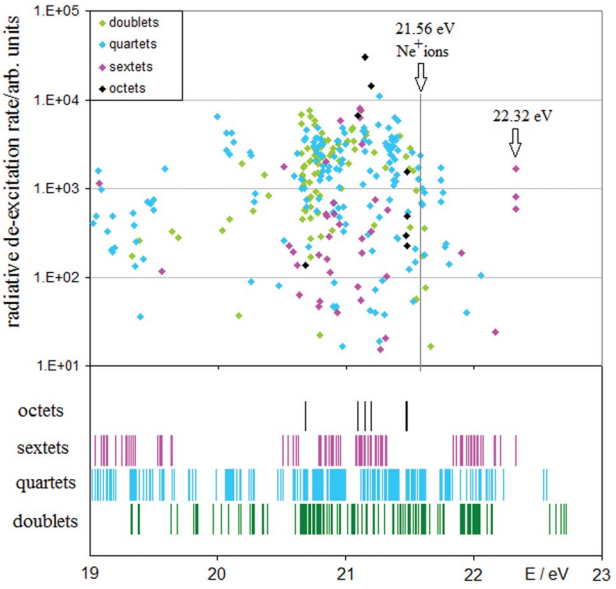

Fig. 10 TR diagram of Fe II in a neon discharge, excitation energies 19–23 eV.

a peak at ≈20.7 eV of the Fe II doublet levels. To determine accurately the relationships between deexcitation rates of levels with different multiplicities in the vicinity of the resonance energy for the Ne^+-ACT reaction, a very good radiometric calibration is needed: the strongly excited octet levels at 21.1–21.2 eV of the term $3d^5(^6S)4p^2\ ^8P$ decay by transitions in the vacuum ultraviolet (VUV) region, the sextet levels by transitions in a wide range from VUV to ≈360 nm, the quartets largely by transitions around 230–240 nm and the doublets mostly by transitions in the visible region around 500 nm. The estimated uncertainty of the radiometric calibration used in this study may be up to ≈30% relative in some narrow wavelength regions. Despite that the plot shown in Fig. 10 gives a reasonably good basic view of the situation.

For comparison with the Fe–Ar^+ ACT reaction, an expanded section of the Fe II TR diagram in an argon discharge is shown in Fig. 11, in the range of 12–16 eV, *i.e.*, spanning over the energy interval width of 4 eV as in the plot shown in Fig. 10. The peak corresponding to Ar^+-ACT (Fig. 11) is much narrower than the energy interval supposedly related to Ne^+-ACT (Fig. 10). This may be largely due to different distributions of Fe II states with suitable multiplicities below the resonance energies for both charge transfer reactions (see Fig. 10 and 11). But, for example, the $3d^54s^2\ d^4P$ term (15.02–15.04 eV) is clearly out of the energy region where the Ar^+-ACT reaction operates, as no lines originating from its levels were observed in the spectrum (these would be lines of the $3d^54s^2\ d^4P$–$3d^6(^5D)4p\ z^4F^\circ$ multiplet, $\lambda \approx$ 771–800 nm).

The sextet states at 22.32 eV with de-excitation rates of 6×10^2 to 1.7×10^3 units in the TR diagram shown in Fig. 10 can be excited by a Ne^+-ACT reaction with metastable iron atoms, in analogy to the reactions (5), (6), occurring in an argon discharge. Full classification of the reacting species is as follows:

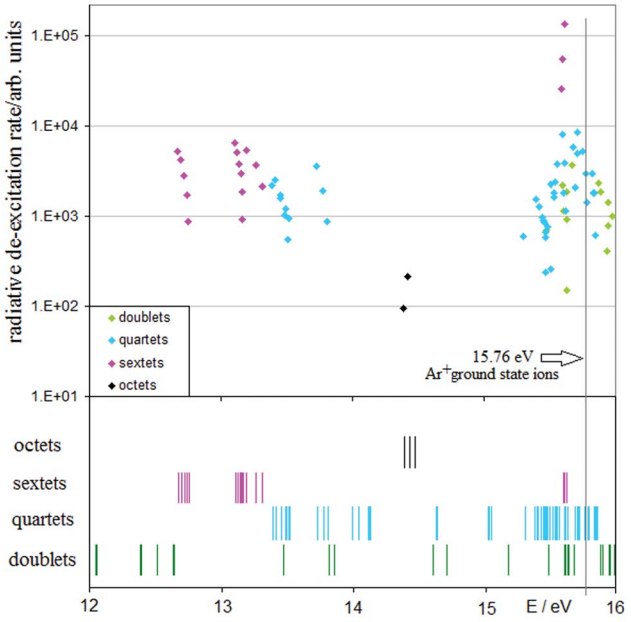

Fig. 11 TR diagram of Fe II in an argon discharge, excitation energies 12–16 eV.

$$\mathrm{Fe^{*}[3d^{7}(^{4}F)4s\ a^{5}F] + Ne^{+}[2s^{2}2p^{5}\ ^{2}P_{3/2}^{\circ}] \rightarrow Fe^{+*}[3d^{5}4s(^{5}S)4d\ ^{6}D] + Ne\ [2s^{2}2p^{6}\ ^{1}S_{0}] + \Delta E} \quad (9)$$

The energy decrement ΔE in reaction (9) is 0.10 eV. Fe II levels below *ca.* 18.5 eV are subject to massive cascade excitation from higher levels. For example, the quartet levels at ≈15.5–16.2 eV have comparable rates of cascade excitation and de-excitation, suggesting that collisional excitation probably plays only a small role for them. Therefore, any considerations concerning collisional excitation in this region must be made with caution and based on net de-excitation rates, *i.e.*, with the cascade excitation rates of these levels subtracted.

This section is to be considered only as an introduction to excitation processes of iron ions in a neon discharge. Further work would be required to obtain a more complete picture.

5. Summary and conclusions

Besides the plots of intensity ratios of emission lines as a function of energy, there are two major tools for describing excitation processes, based on information that can be derived from emission spectra: the TR diagrams and the Boltzmann plots. TR diagrams were defined in Section 2 and Boltzmann plots were mentioned in Section 4.3. It is worthwhile summarizing here their similarities and differences, which is done in Table 3. Boltzmann plots are more useful in describing higher power atmospheric discharges, such as ICP, than a glow discharge, because, at a higher pressure, collisional processes dominate the excitation/de-excitation paths and conditions close to local thermodynamic equilibrium are more likely to occur. The present study uses largely TR diagrams.

The process that dominates the excitation of the Fe II spectrum both in argon and neon glow discharges is the asymmetric charge transfer reaction between ions of the discharge gas and neutral iron atoms. Besides ground state Fe atoms, charge transfer reactions with argon and neon ions were confirmed also for a number of Fe I metastable states. In the case of Ar^{+}-ACT, the Fe I metastables up to the energy of ≈2.9 eV are involved. Sextet levels at ≈15.60 eV are more strongly excited by Ar^{+}–Fe charge transfer, than quartet levels with almost the same energy. There are differences between Ar^{+}–Fe and Ne^{+}–Fe charge transfer reactions, the latter leading to a much wider range of strongly excited Fe II levels (≈20.6–21.6 eV) than the Ar^{+}–Fe reaction (≈15.5–15.9 eV). This is partly due to the distribution of energy levels of appropriate energies and multiplicities. Also, in the neon discharge, a number of strongly excited doublet and octet Fe II states was observed with energies close to the neon ionization energy. If they are excited by Ne^{+}-ACT, it would mean that the Wigner spin rule, according to which the combined spin of reacting particles is conserved, is violated in the Ne^{+}-ACT

Table 3 TR diagrams and Boltzmann plots: an overview

Feature	TR diagrams	Boltzmann plots (excitation functions)
The quantity on abscissa	E_i	E_i
The quantity on ordinate	$\sum_i \lambda_{ik} I_{ik}$, $\sum_k \lambda_{ik} I_{ik}$	$\lambda_{ik} I_{ik}/(g_i A_{ik})$
Ordinate scale	Linear or logarithmic	Logarithmic
The points represent	Levels (or terms)	Observed lines
Type of information displayed	Relative transition rates	Relative populations
Brings information about	Levels (terms)	Upper levels of observed lines
Radiometric intensity calibration	Needed	Needed
Extra information required	None	Transition probabilities Statistical weights of the levels
Suitable for investigating	Selective collisional excitation Cascade processes Radiative population rates	Existence of LTE Excit. temperature if LTE exists
Most useful if	RD ≫ CD[a]	RD ≪ CD[a]

[a] RD = the rate of radiative decay and CD = the rate of collisional de-excitation.

reaction. In an argon discharge, this might concern some doublet Fe II levels close to the argon ionization energy. But their radiative de-excitation rates are by two orders of magnitude lower than those of the most strongly excited levels. The Ar^+-ACT reaction is strongly suppressed by small amounts of hydrogen. This has consequences for analytical methodology, namely, that the strong Fe II lines of the y^6P°–a^6D multiplet, $\lambda =$ 161–163 nm, are very sensitive to the presence of hydrogen, either as an impurity in the argon plasma (from moisture) or coming from the analyzed sample.

Besides charge transfer, also other selective reactions were identified, occurring only at narrow energy intervals. They include Penning excitation of ground state- and metastable Fe^+ ions by argon metastables. All these reactions produce characteristic peaks at the corresponding energies in the TR diagrams.

The lowest levels contributing to Fe II emission spectrum, at energies 12.6–13.8 eV, are probably mainly excited by electronic collisions, besides radiative decay of higher excited states. Contrary to the earlier work by Zhang *et al.*,[13] no evidence was found for any kind of local thermodynamic equilibrium in this energy region. Hence, any 'temperatures', as derived from Fe II glow discharge emission spectra, are meaningless. Prospects to find conditions close to LTE may exist for the lowest (metastable) Fe II levels, the populations of which could be possibly determined by absorption measurements.

The processes mentioned above can satisfactorily explain excitation of the Fe II spectrum in an argon discharge. The Fe II spectrum in a neon glow discharge is much more complex, due to cascade processes (excitation by radiative decay of higher Fe II levels). A detailed study of prospective selective excitation reactions for Fe II levels below *ca.* 18.5 eV in neon discharges would be therefore much more difficult than in argon discharges.

To summarise, the excitation of Fe^+ ions in argon-, neon- and argon–hydrogen glow discharges has been described, based on the formalism of transition rate diagrams. The data presented here can be used as basis for collisional-radiative models of iron in glow discharge plasmas and to compare the predictions of such models with experimental data.

References

1 K. R. Marcus and J. A. C. Broekaert, *Glow Discharge Plasmas in Analytical Spectroscopy*, John Wiley & Sons, Chichester, 2003.
2 R. E. Steiner, C. M. Barshick, A. Bogaerts, Glow Discharge Optical Spectroscopy and Mass Spectrometry, in *Encyclopedia of Analytical Chemistry*, ed.R. A. Meyers, J. Wiley & Sons Ltd, 2009.
3 P. W. J. M. Boumans, *Theory of Spectrochemical Excitation*, Hilger & Watts, London, 1966.
4 S. Amoruso, R. Bruzzese, N. Spinelli and R. Velotta, Characterization of laser ablation plasmas, *J. Phys. B: At., Mol. Opt. Phys.*, 1999, **32**, R131.
5 H. Haraguchi, T. Hasegawa and M. Abdullah, Inductively coupled plasmas in analytical atomic spectrometry: excitation mechanisms and analytical feasibilities, *Pure Appl. Chem.*, 1988, **60**, 685.
6 Z. Weiss, Glow discharge excitation and matrix effects in the Zn–Al–Cu system in argon and neon, *Spectrochim. Acta, Part B*, 2007, **62**, 787.
7 E. B. M. Steers and J. Fielding, Charge-transfer excitation processes in the Grimm lamp, *J. Anal. At. Spectrom.*, 1987, **2**, 239.
8 E. B. M. Steers and A. Thorne, Application of high resolution Fourier transform spectrometry to the study of glow discharge sources. 1. Excitation of iron and chromium spectra in a microwave-boosted glow discharge source, *J. Anal. At. Spectrom.*, 1993, **8**, 309.
9 S. Mushtaq, E. B. M. Steers, J. C. Pickering and K. Putyera, Selective and non-selective excitation/ionization processes in analytical glow discharges: excitation of the ionic spectra in argon–helium mixed plasmas, *J. Anal. At. Spectrom.*, 2014, **29**, 681.
10 G. C.-Y. Chan and G. M. Hieftje, Using matrix effects as a probe for the study of the charge-transfer mechanism in inductively coupled plasma-atomic emission spectrometry, *Spectrochim. Acta, Part B*, 2004, **59**, 163.
11 K. Wagatsuma, R. Oka and S. Urushibata, Excitation processes in introduction of bias current to a radio-frequency glow discharge plasma evaluated from Boltzmann plots of iron atomic and ionic spectral lines, *Anal. Sci.*, 2012, **28**, 759.
12 L. Zhang, S. Kashiwakura and K. Wagatsuma, Boltzmann statistical consideration on the excitation mechanism of iron atomic lines emitted from glow discharge plasmas, *Spectrochim. Acta, Part B*, 2011, **66**, 785.
13 L. Zhang, S. Kashiwakura and K. Wagatsuma, Deviation from Boltzmann distribution in excited energy levels of singly-ionized iron in an argon glow discharge plasma for atomic emission spectrometry, *Spectrochim. Acta, Part B*, 2012, **67**, 24.
14 Z. Weiss, E. B. M. Steers, J. C. Pickering and S. Mushtaq, Transition rate diagrams—A new approach to the study of selective excitation processes: The spectrum of manganese in a Grimm-type glow discharge, *Spectrochim. Acta, Part B*, 2014, **92**, 70.
15 S. Johansson and U. Litzén, Possibilities of obtaining laser action from singly ionised iron group elements through charge transfer in hollow cathode lasers, *J. Phys. B: At. Mol. Phys.*, 1980, **13**, L253.
16 E. B. M. Steers and J. Leis, Excitation of the spectra of neutral and singly ionized atoms in the Grimm-type discharge lamp, with and without supplementary microwave excitation, *Spectrochim. Acta, Part B*, 1991, **46**, 527.
17 K. Wagatsuma and K. Hirokawa, Classification of singly ionized iron emission lines in the 160–250 nm wavelength region from Grimm-type glow discharge plasma, *Spectrochim. Acta, Part B*, 1996, **51**, 349.
18 E. B. M. Steers, P. Šmíd and Z. Weiss, Asymmetric charge transfer with hydrogen ions—an important factor in the "hydrogen effect" in glow discharge optical emission spectroscopy, *Spectrochim. Acta, Part B*, 2006, **61**, 414.
19 P. Šmíd, E. B. M. Steers, Z. Weiss, J. Pickering and V. Hoffmann, The effect of hydrogen and nitrogen on

emission spectra of iron and titanium atomic lines in analytical glow discharges, *J. Anal. At. Spectrom.*, 2008, **23**, 1223.

20 S. Johansson, *Phys. Scr.*, 2009, **T134**, 014013, DOI: 10.1088/0031–8949/2009/T134/014013.

21 G. Nave and S. Johansson, The spectrum of Fe II, *Astrophys. J., Suppl. Ser.*, 2013, 204.

22 I. Korolov, G. Bánó, Z. Donkó, A. Derzsi and P. Hartmann, Experimental study of the asymmetric charge transfer reaction between Ar^+ ions and Fe atoms, *J. Chem. Phys.*, 2011, **134**, 064308.

23 Z. Weiss, Emission yields and the standard model in glow discharge optical emission spectroscopy: links to the underlying physics and analytical interpretation of the experimental data, *Spectrochim. Acta, Part B*, 2006, **61**, 121.

24 J. C. Pickering, High resolution Fourier transform spectroscopy with the Imperial College (IC) UV-FT spectrometer, and its applications to astrophysics and atmospheric physics: a review, *Vib. Spectrosc.*, 2002, **29**, 27.

25 A. Thorne, U. Litzén and S. Johansson, *Spectrophysics: Principles and Applications*, Springer, 1999.

26 J. C. Pickering, S. Johansson and P. L. Smith, The FERRUM project: Branching ratios and atomic transition probabilities of Fe II transitions from the $3d^6(a^3F)4p$ subconfiguration in the visible to VUV spectral region, *Astron. Astrophys.*, 2001, **377**, 361.

27 S. D. Bergeson, K. L. Mullman, M. E. Wickliffe, J. E. Lawler, U. Litzén and S. Johansson, Branching fractions and oscillator strengths for Fe II transitions from the $3d^6(^5D)4p$ subconfiguration, *Astrophys. J.*, 1996, **464**, 1044.

28 A. Kramida, Yu. Ralchenko, J. Reader and NIST ASD Team, *NIST Atomic Spectra Database (ver. 5.1)*, National Institute of Standards and Technology, Gaithersburg, MD, 2013, http://www.physics.nist.gov/asd, May 10 2014.

29 T. R. O'Brian, M. E. Wickliffe, J. E. Lawler, W. Whaling and J. W. Brault, Lifetimes, transition probabilities and level energies in Fe I, *J. Opt. Soc. Am. B*, 1991, **8**, 1185.

30 Z. Weiss, E. B. M. Steers, P. Šmíd and V. Hoffmann, Towards a catalogue of glow discharge emission spectra, *J. Anal. At. Spectrom.*, 2009, **24**, 27.

31 N. Jakubowski, E. Steers and A. Tempez, Glow and Glory, *J. Anal. At. Spectrom.*, 2007, **22**, 715.

32 K. Marshall, P. M. Willis, Centered Sphere Spectrometer, US Patent 6023330, 1998.

33 J. R. Fuhr and W. L. Wiese, A critical compilation of atomic transition probabilities for atomic and singly ionized iron, *J. Phys. Chem. Ref. Data*, 2006, **35**, 1669.

34 Z. Weiss, E. B. M. Steers and P. Šmíd, Excitation of zinc in a Grimm-type glow discharge: effects of hydrogen and other excitation-related matrix effects, *J. Anal. At. Spectrom.*, 2005, **20**, 839.

35 P. H. Ratcliff and W. W. Harrison, The effect of water vapor in glow discharge mass spectrometry, *Spectrochim. Acta, Part B*, 1994, **49**, 1747–1757.

36 V.-D. Hodoroaba, V. Hoffmann, E. B. M. Steers and K. Wetzig, Emission spectra of copper and argon in an argon glow discharge containing small quantities of hydrogen, *J. Anal. At. Spectrom.*, 2000, **15**, 951.